On-site education of VEGF-recruited monocytes improves their performance as angiogenic and arteriogenic accessory cells

Inbal Avraham-Davidi,[1] Simon Yona,[2] Myriam Grunewald,[1] Limor Landsman,[2] Clement Cochain,[3] Jean Sebastien Silvestre,[3] Haim Mizrahi,[1] Mohammad Faroja,[4] Dalit Strauss-Ayali,[2] Matthias Mack,[5] Steffen Jung,[2] and Eli Keshet[1]

[1]Department of Developmental Biology and Cancer Research, the Hebrew University-Hadassah Medical School, Jerusalem 91120, Israel
[2]Department of Immunology, Weizmann Institute of Science, Rehovot 76100, Israel
[3]PARCC-Institut National de la Santé et de la Recherche Médicale U970, 75737 Paris, Cedex 15, France
[4]Deptment of Surgery, Hadassah Medical Center, Jerusalem 91120, Israel
[5]Department of Internal Medicine, University of Regensburg, 93053 Regensburg, Germany

Adult neovascularization relies on the recruitment of monocytes to the target organ or tumor and functioning therein as a paracrine accessory. The exact origins of the recruited monocytes and the mechanisms underlying their plasticity remain unclear. Using a VEGF-based transgenic system in which genetically tagged monocytes are conditionally summoned to the liver as part of a VEGF-initiated angiogenic program, we show that these recruited cells are derived from the abundant pool of circulating Ly6C^{hi} monocytes. Remarkably, however, upon arrival at the VEGF-induced organ, but not the naive organ, monocytes undergo multiple phenotypic and functional changes, endowing them with enhanced proangiogenic capabilities and, importantly, with a markedly increased capacity to remodel existing small vessels into larger conduits. Notably, monocytes do not differentiate into long-lived macrophages, but rather appear as transient accessory cells. Results from transfers of presorted subpopulations and a novel tandem transfer strategy ruled out selective recruitment of a dedicated preexisting subpopulation or onsite selection, thereby reinforcing active reprogramming as the underlying mechanism for improved performance. Collectively, this study uncovered a novel function of VEGF, namely, on-site education of recruited "standard" monocytes to become angiogenic and arteriogenic professional cells, a finding that may also lend itself for a better design of angiogenic therapies.

CORRESPONDENCE
Steffen Jung:
s.jung@weizmann.ac.il
OR
Eli Keshet:
elik@ekmd.huji.ac.il

Abbreviations used: CCR2, C-C chemokine receptor 2; CX_3CR1, fractalkine receptor; EPC, endothelial progenitor cell; MMP8, matrix metalloproteinase-8; PKH26, red fluorescent cell linker; tTA, tetracycline-regulated transactivator; VEGF, vascular endothelial growth factor.

Unlike developmental neovascularization that makes extensive use of resident mesenchymal progenitor cells (angioblasts), adult neovascularization typically takes place via sprouting angiogenesis, as the pool of tissue angioblasts has been exhausted by adulthood. Likewise, the relative contribution of bone marrow–derived endothelial progenitor cells (EPCs) to the neovasculature is still debated and may vary in different experimental settings (Ruzinova et al., 2003; Peters et al., 2005; Purhonen et al., 2008) Adult angiogenesis is mediated by locally induced angiogenic factors, primarily VEGF, but is also assisted by complementary activities by myeloid cells, recruited to the angiogenic site in a process known as cell-assisted angiogenesis (Lin et al., 2001; De Palma et al., 2003; Grunewald et al., 2006; Jin et al., 2006). In a tumor milieu, for example, the essential proangiogenic role played by recruited monocytes and intratumoral macrophages has been demonstrated using different approaches to prevent their recruitment, as well as by their

I. Avraham-Davidi and S. Yona contributed equally to this paper.
S. Yona's present address is Division of Medicine, University College London, London, WC1E 6JF, England, UK.

The Rockefeller University Press $30.00
J. Exp. Med. 2013 Vol. 210 No. 12 2611-2625
www.jem.org/cgi/doi/10.1084/jem.20120690

on-site ablation (De Palma et al., 2003; De Palma et al., 2005; Lin et al., 2006). Refractoriness of the tumor vasculature to VEGF inhibition has been attributed to compensatory factors provided by recruited myeloid cells (Shojaei et al., 2007, 2009).

Most, if not all angiogenic responses in the adult are promoted by VEGF, which is either induced as a result of stochastic genetic changes in tumors or by environmental cues, primarily hypoxia. The incidental nature of VEGF induction has prompted the proposition that recruitment of accessory cells might be required for efficient VEGF-initiated neovascularization. Indeed, we have previously shown that an ongoing VEGF stimulus is required for perivascular positioning of incoming monocytes and for their retention in this strategic location from which they can exert a paracrine accessory role (Grunewald et al., 2006).

Extravasated monocytes were shown to participate in the process of arteriogenesis, i.e., remodeling of existing small vessels into larger vessels via promotion of in-wall proliferation of endothelial cells, in the context of the compensatory response to vessel occlusion (collateralization) (Cai and Schaper, 2008). However, the proposition that monocytes summoned by VEGF foster the generation of large conduits as an indispensable part of a natural, VEGF-promoted adult neovascularization requires further study.

Monocytes represent a most versatile and dynamic cell population composed of subsets that differ in phenotype, size, and morphology and gene expression profiles (Geissmann et al., 2003; Ingersoll et al., 2010). Originating in the bone marrow and released to the peripheral circulation as short-lived, nondividing cells, monocytes are believed to serve as a transient reservoir of myeloid precursors that can be summoned to sites of injury to aid in the maintenance of tissue homeostasis. Two discrete subsets of blood monocytes have been identified, distinguishable in the mouse by their membrane expression of Ly6C and the chemokine receptor CCR2 (Geissmann et al., 2003; Palframan et al., 2001). Adoptive transfers of $Ly6C^{lo}$ and $Ly6C^{hi}$ blood monocytes established that the two subsets differ with respect to their respective fate and function in the periphery (Geissmann et al., 2003; Landsman and Jung, 2007; Varol et al., 2009). $Ly6C^{hi}$ monocytes are efficiently recruited to sites of inflammation, but in absence of the latter give rise to $Ly6C^{lo}$ cells (Varol et al., 2007). $Ly6C^{lo}$ monocytes have been proposed to be involved in tissue remodeling, e.g., after myocardial infarction, and to replenish resident macrophage populations (Arnold et al., 2007; Landsman and Jung, 2007; Nahrendorf et al., 2007).

Given the heterogeneity of monocytes and their descendants, the question arises whether proangiogenic and proarteriogenic monocytes recruited by VEGF represent a preexisting subpopulation committed to perform these specialized functions in the periphery. Alternatively, acquisition of these properties could reflect post-recruitment education governed by cues prevailing in the particular tissue milieu. In the case of pro-angiogenic Tie2-expressing monocytes (TEMs), for example, it has been suggested on the basis of gene expression signature kinships that they represent a monocyte subset committed to perform a distinct, pro-angiogenic extravascular function in the tumor microenvironment (Pucci et al., 2009).

The notion of macrophage education has been proposed to explain the multiple, often opposing functions of tumor-associated macrophages (TAMs; Qian and Pollard, 2010). Thus, polarized expression of either pro- or antitumor functions has been argued to result from inherent macrophage plasticity and to be determined by the particular microenvironmental signals the cells are exposed to, culminating in selective tuning of TAM functions within a spectrum encompassing the M1 and M2 extremes (Sica et al., 2008). Yet, given the complexity of the tumor microenvironment, it has been difficult to exclude alternative mechanisms generating functional heterogeneity, including preexisting minor populations, selective and/or sequential recruitment or on-site variant selection. Moreover, it remained possible that extravasated monocytes do not necessarily need to differentiate into macrophages but might fulfill these specialized functions in the periphery as short-lived, reprogrammed monocytes.

To distinguish between different mechanisms responsible for generating angiogenic and arteriogenic monocytes, we took advantage of a unique transgenic system that allows conditional summoning of genetically tagged monocytes by VEGF to a target organ of choice and subsequently retrieving them for analysis of changes in gene expression and functional performance.

RESULTS

A conditional transgenic system for organ-specific recruitment of monocytes by VEGF

To analyze monocytes recruited to sites of VEGF-initiated, ongoing neovascularization, we took advantage of a transgenic model in which VEGF expression is conditionally induced in the organ of choice in a reversible manner (see Materials and methods for details). We previously used this system to show that VEGF selectively recruits circulating monocytes to the organ from which it emanates and retains the extravasated cells around activated vessels (Grunewald et al., 2006). In this study, we focused on the monocytes summoned by VEGF to the adult liver by using a liver-specific promoter (P-LAP) that drives expression of the tetracycline-regulated transactivator (tTA) transgene. The liver was chosen because it is more suitable than other organs for retrieval of sufficient quantities of newly recruited monocytes for further analyses. To provide a convenient marker for enumerating and sorting recruited monocytes, P-LAP-tTA^+/tet-$VEGF^+$ mice were crossed with animals harboring a knock-in transgene encoding a GFP reporter under the CX_3CR1 chemokine receptor promoter, thus creating a triple transgenic P-LAP-tTA^+/tet-$VEGF^+$:$CX_3CR1^{GFP/+}$ mouse. CX_3CR1 promoter activity is by large restricted to the mononuclear myeloid lineage, including all BM and circulating $CD115^+$ monocytes (Jung et al., 2000; Geissmann et al., 2003). VEGF was induced in mature 6–8 wk old mice by withdrawal of tetracycline from the drinking water ($VEGF^{ON}$) and blood

samples were monitored for the efficiency of VEGF induction and to select mice in which the VEGF switch worked efficiently (manifested by circulating VEGF levels of >650 pg/ml compared with <40 pg/ml detected in $VEGF^{OFF}$ mice). A time point of 14 d after VEGF induction was chosen for initial analysis of recruited monocytes because at this time a robust angiogenic response in the liver was still ongoing, associated with a marked accumulation of monocytes in the VEGF-induced organ. A modest decline in the BM compartment and corresponding increase in the circulation suggested BM monocyte mobilization to the blood. The most dramatic effect of VEGF, however, was the monocyte recruitment to the liver as indicated by the specific accumulation of GFP^+ cells (Fig. 1 a). Corroborating our previous results, the majority of extravasated liver monocytes came to reside in close proximity to blood vessels, a site compatible with their proposed paracrine accessory role (Fig. 1 b).

Monocytes recruited by VEGF are $Ly6C^{hi}$ monocytes but dynamically change their surface markers after entrapment in the target organ

Analysis of characteristic myeloid surface markers established that GFP^+ resident myeloid cells in $VEGF^{OFF}$ livers were clearly distinct from the recruited population in $VEGF^{ON}$ mice (Fig. 2 a). Notably, although VEGF induced in the liver is accessible to the systemic circulation, blood monocytes from either $VEGF^{OFF}$ or $VEGF^{ON}$ animals retained the subset distribution into $Ly6C^{hi}$ and $Ly6C^{lo}$ cells and were indistinguishable by the surface markers tested (Fig. S1).

To determine which of the reported monocyte subsets is recruited to the $VEGF^{ON}$ liver and to investigate potential VEGF-effects on the recruited cells, we resorted to adoptive transfers of fluorescently tagged monocytes. This procedure discriminates between monocytes recruited by VEGF from the resident myeloid pool. One day following transfer of CX_3CR1^{GFP} monocytes, grafted $Ly6C^{hi}$ and $Ly6C^{lo}$ monocytes were readily detected in the recipient blood (Fig. 2 b). As reported previously (Varol et al., 2007), $Ly6C^{hi}$ monocytes converted with time into $Ly6C^{lo}$ monocytes. Congruent with the observations in the P-LAP-tTA^+/tet-$VEGF^+$:CX_3CR1^{GFP} mice (Fig. 1 a), adoptively transferred CX_3CR1^{GFP} monocytes homed to P-LAP-tTA^+/tet-$VEGF^{+/ON}$ livers in much larger numbers than to the naive liver (data not shown), thus substantiating the notion that the VEGF milieu entraps circulating monocytes. Remarkably, whereas $Ly6C^{hi}$ monocytes retained Ly6C expression in the $VEGF^{OFF}$ liver, they down-regulated Ly6C expression in the $VEGF^{ON}$ liver in a time-dependent manner (Fig. 2 b). Similarly to what had been observed for endogenous myeloid cells in $VEGF^{ON}$ livers (Fig. 2 a), also grafted monocyte-derived cells in the $VEGF^{ON}$ liver, but not the $VEGF^{OFF}$ liver up-regulated CD64 and F4/80 expression (Fig. 2 c).

To further determine which of the reported monocyte subsets is recruited to the $VEGF^{ON}$ livers we next performed an adoptive transfer of highly purified $Ly6C^{hi}$ monocytes. As shown in Fig. 2 d, these cells efficiently homed to the VEGF-induced liver and converted therein into $Ly6C^{lo}$ cells, suggesting that VEGF-recruited monocytes in this model are exclusively of the $Ly6C^{hi}$ type. To corroborate this conclusion we resorted to a monocyte ablation strategy that specifically targets $Ly6C^{hi}$ cells by virtue of their CCR2 expression. In brief, concomitantly with switching-on VEGF expression in P-LAP-tTA^+/tet-$VEGF^+$:CX_3CR1^{GFP} mice, $Ly6C^{hi}$ monocytes were depleted via daily injection of the anti-CCR2 mAb MC21 (Mack et al., 2001), throughout the 11-d induction period. MC21 injections led to the efficient selective depletion of $CCR2^+$ $Ly6C^{hi}$ monocytes from the circulation whereas $CCR2^-$ $Ly6C^{lo}$ cells were spared (Fig. 2 e). Remarkably, this treatment completely abrogated monocyte infiltration of the VEGF-induced livers (Fig. 2 f), establishing that in this experimental model VEGF-recruited monocytes are exclusively of the $Ly6C^{hi}$ type.

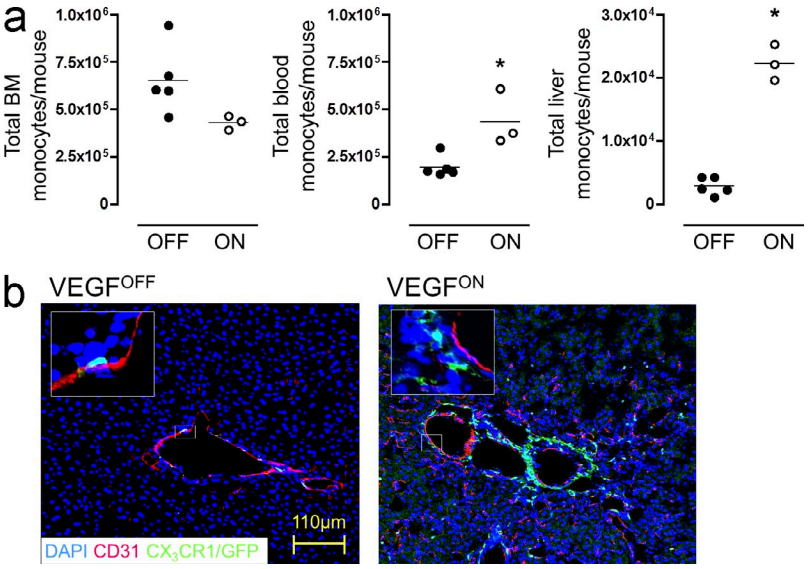

Figure 1. VEGF recruits circulating monocytes to a perivascular site in the angiogenic liver. (a) VEGF expression was induced in the liver of P-LAP-tTA^+/tet-$VEGF^+$:$CX_3CR1^{GFP/+}$ mice as described in the Materials and methods. BM, circulating, and liver monocytes, identified as $CX_3CR1^{GFP/+}$, $CD115^+$, and $CD11b^+$ triple-positive cells, were analyzed by flow cytometry after 2 wk of VEGF induction. Total numbers of monocytes in the respective organs were compared with those detected in mice maintained in the $VEGF^{OFF}$ mode. Each data point represents an individual animal ($n = 3–5$), and the experiment was performed twice. *, $P < 0.05$ versus OFF mice. (b) Immunofluorescence micrographs of livers from $VEGF^{OFF}$ and $VEGF^{ON}$ P-LAP-tTA^+/tet-$VEGF^+$:$CX_3CR1^{GFP/+}$ mice. Endothelial cells were highlighted by CD31 staining (red), whereas monocytes are identified on the basis of GFP positivity. Enlarged views of the insets further illustrate perivascular positioning of the large number of monocytes recruited by VEGF. Representative image of $n = 3$ mice per group performed twice.

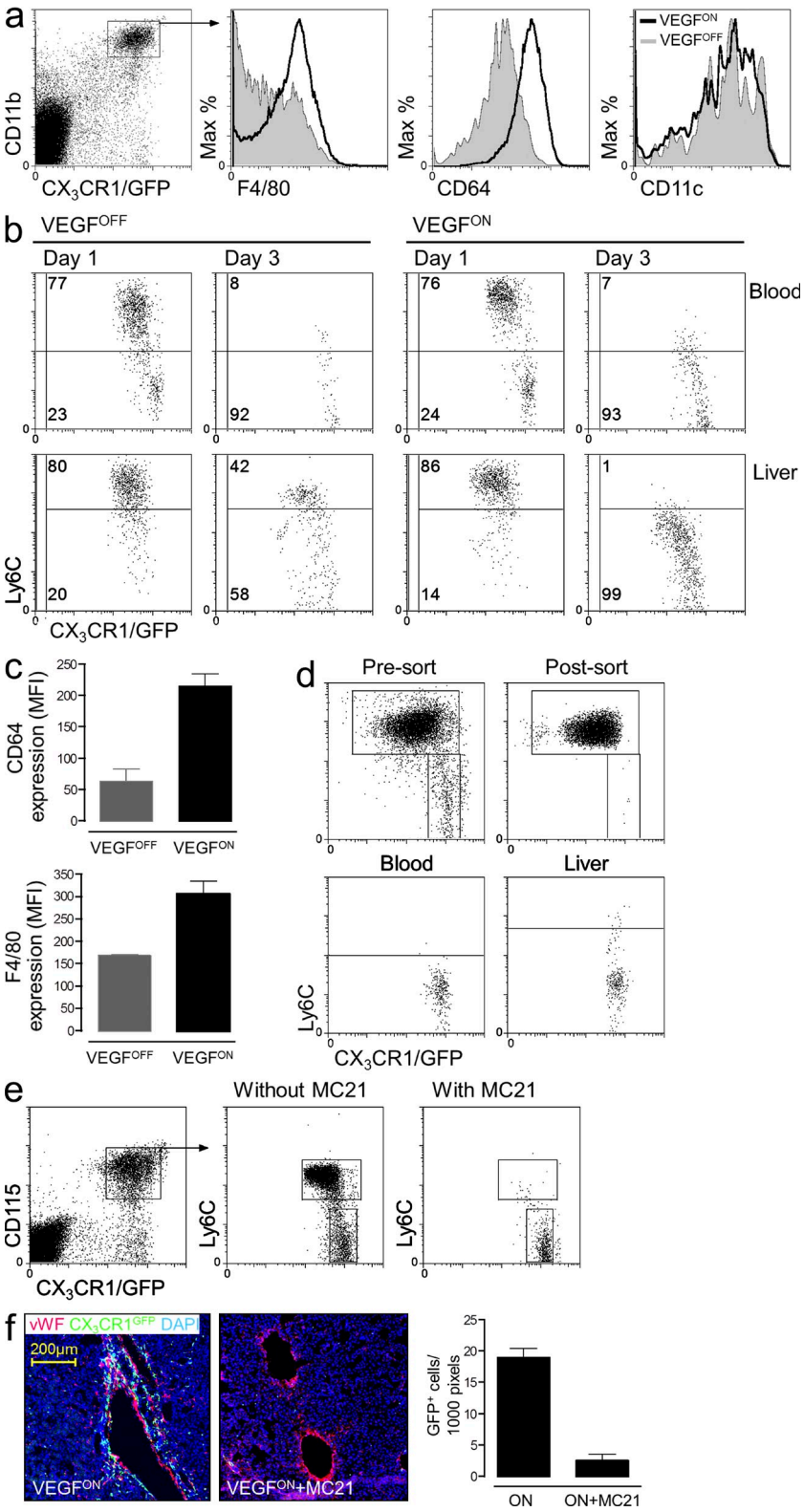

Figure 2. Monocytes recruited by VEGF are Ly6C^{hi} monocytes that dynamically change their surface markers after entrapment in the target organ. (a) Flow cytometry analysis of CX_3CR1^{GFP}-positive myeloid cells retrieved as described above from the livers of VEGF^{ON} and VEGF^{OFF} mice with respect to expression of the indicated surface markers. Representative of $n = 3$ mice per group and performed twice. (b) Adoptive transfer of ~1.5 × 10^6 $CX_3CR1^{GFP/+}$ BM monocytes to 6–8-wk-old P-LAP-tTA$^+$/tet-VEGF$^+$ mice in which hepatic expression of VEGF was induced 2 wk earlier. Grafted cells from the liver and from the blood of recipient mice were analyzed for their Ly6C expression 1 or 3 d later. Representative dot plot of $n = 2$–4 mice per group performed three times. (c) Mean expression levels of CD64 and F4/80 on adoptively transferred monocytes retrieved from VEGF^{OFF} and VEGF^{ON} livers. Data from three independent experiments with $n = 3$ mice per group. (d) Ly6C^{hi} $CX_3CR1^{GFP/+}$ BM monocytes were purified to 99% homogeneity through capture on CD115-coated magnetic beads followed by FACS sorting. Isolated cells were analyzed for their purity and adoptively transferred to VEGF^{ON} mice. 3 d after the transfer, grafted cells from the blood and the livers of recipient mice were analyzed for Ly6C expression. Representative dot plots of $n = 3$ mice per group performed twice. (e) Circulating Ly6C^{hi} monocytes were depleted by daily injections of the mAb MC21 for 10 d in P-LAP-tTA$^+$/tet-VEGF$^+$:$CX_3CR1^{GFP/+}$ starting 1 d before the induction of VEGF. Note selective elimination of Ly6C^{hi}, but not of Ly6C^{lo} monocytes from the circulation. Representative dot plots of $n = 2$–3 mice per group and performed twice. (f) Immunofluorescence micrographs of liver sections from control- and MC21-treated mice with an ongoing VEGF on switch. This reduction in monocyte influx was quantified by counting the mean number of $CX_3CR1^{GFP/+}$ cells per 1,000 pixels of vWF$^+$ blood vessels. Representative image of $n = 2$–3 mice per group and performed twice.

The spleen may serve as a reservoir of Ly6C^{hi} monocytes as was indeed shown using a myocardial ischemia mouse model (Swirski et al., 2009). To determine whether the splenic reservoir may also contribute to VEGF-induced monocyte recruitment in our model, we performed splenectomy before switching on hepatic VEGF expression. There was no difference in the number of recruited monocytes and no difference in the neovascularization response (unpublished data). We

conclude that there is no significant contribution in our experimental system by the splenic reservoir.

Recruited Ly6C^{hi} monocytes are short-lived and phenotypic changes take place by VEGF education

Upon entry into tissues, monocytes typically spontaneously differentiate into persisting tissue macrophages. Surprisingly, however, the analysis of the P-LAP-tTA^{+}/tet-VEGF^{+} monocyte recipients revealed that the cells only transiently populated the VEGF^{ON} livers, as graft-derived cells waned with time and disappeared altogether by day 7 after transfer (Fig. 3 a).

To determine whether the apparent disappearance of recruited monocytes is caused by apoptotic death or, alternatively, caused by their return into the circulation, we performed flow cytometric analysis of cells retrieved from the VEGF-induced liver using the cell death markers Annexin V and Sytox. Results showed that whereas adoptively transferred circulating monocytes exhibited only a constant low rate of cell death, monocytes recruited to the liver showed a high level of apoptotic cell death dramatically increasing between day 1 and 3 from transfer (Fig. 3 b), thus arguing that apoptosis is the mechanism responsible for the transient presence of recruited monocytes in the VEGF-induced organ.

The short half-life of VEGF-recruited monocytes, together with the finding that their phenotypic change is acquired within 3 d after their entry into the liver argues against on-site selection of a preexisting subpopulation as a mechanism accounting for apparent phenotypic change. Indeed, CSFE dilution experiments showed that by 3 d, grafted monocytes have not divided (Fig. 3 c). Likewise, the possibility of selective recruitment by VEGF of a minor subpopulation expressing different markers than the bulk of circulating monocytes was ruled-out by demonstrating a similar phenotypic conversion of a homogenous grafted population of Ly6C^{hi} monocytes (Fig. 2 d). Thus, these data support a mechanism of reprogramming (education) as the underlying mechanism for change, and the fact that it takes place only in the VEGF-induced organ indicate VEGF-instructed education.

Monocytes recruited by VEGF are also required for circumferential enlargement of existing vessels

The ability to completely inhibit monocyte recruitment by preventing Ly6C^{hi} monocytes from reaching the VEGF-induced liver (Fig. 2 f) enabled us to investigate functional aspects of the cells. We previously demonstrated the significant contribution of myeloid cells to VEGF-driven angiogenesis (Grunewald et al., 2006). Here, we wished to determine

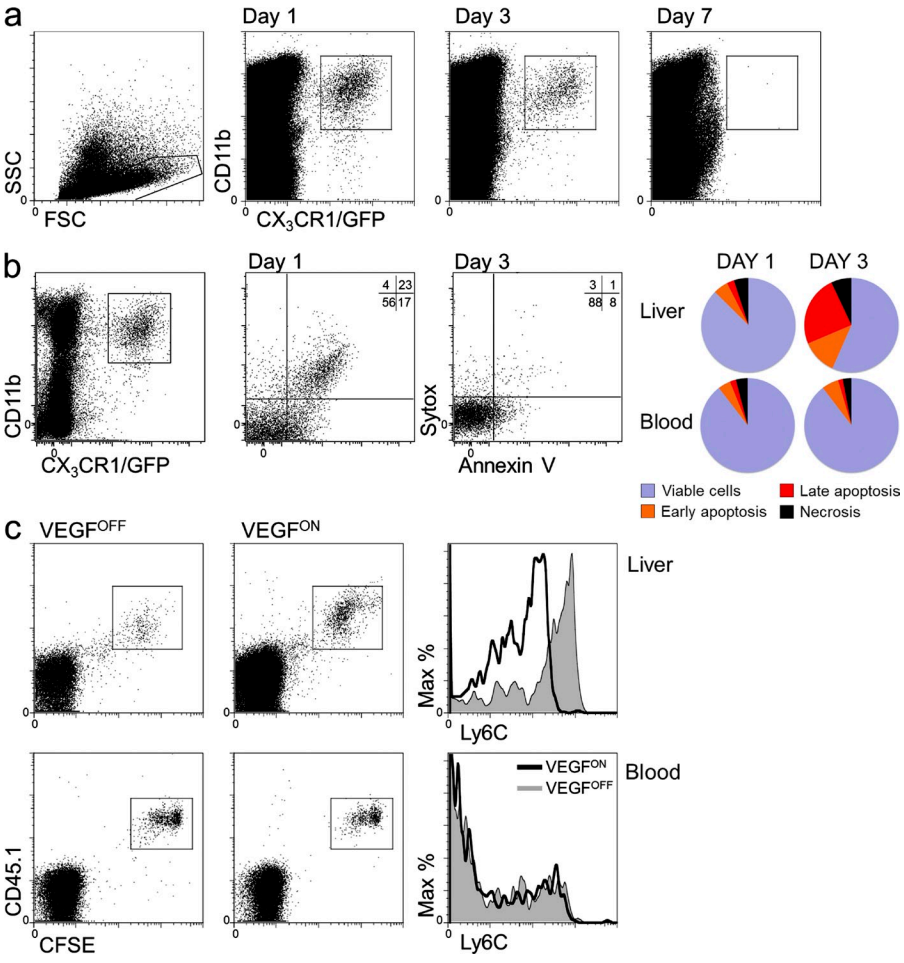

Figure 3. VEGF-recruited monocytes are short-lived. (a) BM CD115^{+} monocytes were isolated from CX$_3$CR1$^{GFP/+}$ donor mice and transferred to VEGF^{ON} mice. 1, 3, and 7 d after monocyte transfer, grafted cells from the livers of recipient mice were analyzed, and adoptively transferred cells were identified as having CD11b^{+} and GFP^{+} expression. Representative dot plots of $n = 2$ mice per time point per group, performed twice. (b) Monocytes retrieved as described in a at days 1 and 3 after transfer were analyzed by flow cytometry using Annexin V and Sytox and compared with monocytes retrieved from the circulation of the same mice. Representative of three independent individual mice per time point. (c) BM monocytes isolated from CD45.1 donor mice were labeled with the intracellular fluorescent dye CFSE before their transfer to VEGF^{OFF} or VEGF^{ON} mice. 3 d after their transfer, CSFE-labeled cells retrieved from the liver or blood of recipient mice were analyzed by flow cytometry for CFSE and Ly6C expression. Note that there was no dilution of CSFE in monocytes from liver relative to monocytes from blood. Representative of $n = 3$ mice per group and performed twice.

whether VEGF-recruited monocytes also contribute to in-wall proliferation of endothelial cells, a process leading to increased diameter of established vessels and constituting a key step in arterialization. Ongoing EC proliferation in existing vessels was visualized by measuring BrdU-positive cells residing in the inner layer of lumenized vascular structures. In contrast to VEGF^{OFF} controls, where BrdU^{+} cells were rarely detected (not depicted), robust EC proliferation was detected in VEGF^{ON} livers, frequently in cells arranged in tandem within the endothelium lining large vessels (Fig. 4 a). A similar configuration of proliferating ECs, indicative of vessel remodeling rather than sprouting angiogenesis, was also detected using Ki67 immunostaining (unpublished data). The overall number of proliferating ECs was significantly reduced in the VEGF^{ON} liver from which Ly6C^{hi} monocytes had been depleted. Notably, the effect of the Ly6C^{hi} monocyte depletion on EC proliferation was more pronounced in the context of large vessels (Fig. 4 b). The latter result suggests that VEGF-recruited monocytes significantly contribute to formation of larger conduits during neovascularization, a result corroborated by experiments described below using grafted monocytes in a surrogate arteriogenesis assay.

VEGF education improves both angiogenic and arteriogenic performance of recruited monocytes. To determine

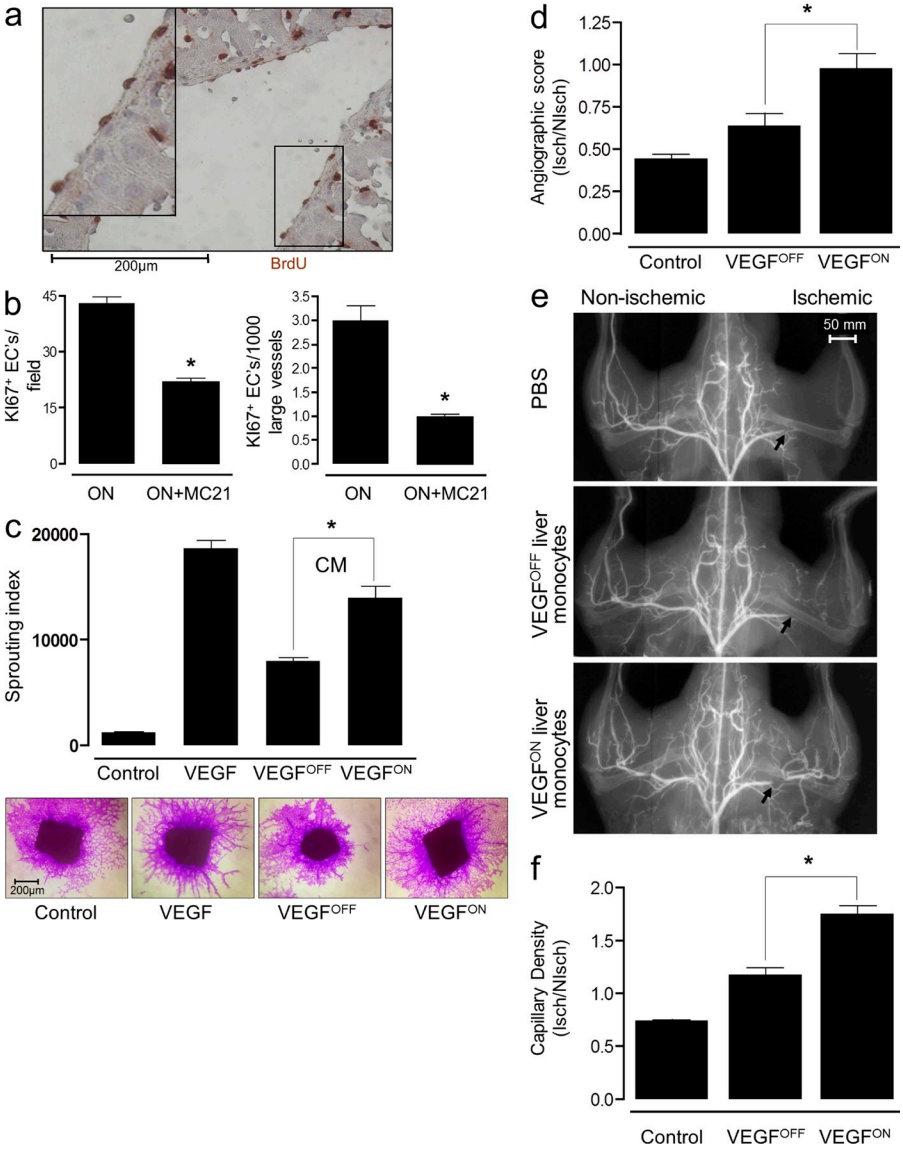

Figure 4. VEGF education enhances both angiogenic and arteriogenic performance of recruited monocytes. (a) Endothelial cell proliferation in VEGF^{ON} (P-LAP-tTA^{+}/tet-VEGF^{+}) mice was visualized using BrdU immunohistochemistry. Representative $n = 3$ mice per group, performed twice. (b) Effects of MC21 treatment on VEGF-induced EC proliferation was measured as described above scoring proliferating EC by Ki67 immunostaining. Representative of $n = 3$ mice per group, performed twice. *, $P < 0.05$ versus ON mice alone. (c) Mouse aortic segments were embedded in collagen and overlaid with a serum-free control medium, serum-free medium containing 10 ng/ml VEGF, or serum-free medium conditioned by monocytes retrieved from VEGF^{OFF} or VEGF^{ON} livers. Equal numbers of monocytes retrieved from VEGF^{OFF} or VEGF^{ON} livers were used to obtain the conditioned media. Capillary sprouts were visualized by crystal violet staining and the mean length of capillary sprouts was measured. CM, conditioned medium. Representative of $n = 4$ mice group, performed three times. *, $P < 0.05$ versus OFF cells. (d–f) Mice underwent right femoral artery ligation and the effects of intraorbitally injected liver VEGF^{OFF}, VEGF^{ON} monocytes (CD11b^{+} cells), or vehicle, angiogenic (f) and arteriogenic (d and e) responses were compared. *, $P < 0.05$ versus OFF cells. Representative of $n = 6$ mice per group, performed three times. (d and e) Arteriogenic response in the proximal region downstream of the ligation site (marked by an arrow in e) of the same animals was evaluated by microangiography. Representative microangiograms are shown in e and angiographic scores are shown in f, $n = 6$ mice per group, performed three times. *, $P < 0.05$ versus OFF cells. (f) Angiogenic response in the gastrocnemius muscle was evaluated by counting fibronectin-positive capillaries in both the ligated and contralateral limb. Results are expressed as ischemic to nonischemic microvascular density ratio. Representative of $n = 6$ mice per group, performed three times.

whether VEGF education results in improved performance of recruited monocytes, as angiogenic accessory cells, we compared proangiogenic activities of educated monocytes with that of naive monocytes using two independent angiogenic assays. First, medium conditioned by CD11b$^+$ cells retrieved from livers of P-LAP-tTA$^+$/tet-VEGF^{OFF} mice was compared with that obtained from P-LAP-tTA$^+$/tet-VEGF^{ON} mice in respect to the induction of sprouting angiogenesis in the aorta ring assay. Conditioned medium from CD11b$^+$ cells representing VEGF-educated monocytes induced sprouting angiogenesis significantly better than medium conditioned by resident CD11b$^+$ cells retrieved from the naive organ (Fig. 4 c). Second, CD11b$^+$ cells retrieved from either WT livers of P-LAP-tTA$^+$/tet-VEGF^{OFF} mice and P-LAP-tTA$^+$/tet-VEGF^{ON} mice were injected into the circulation of mice in which hind limb ischemia had been induced by femoral artery ligation. In this system, ensuing hypoxia triggers an angiogenic response in the distal region of the gastrocnemius muscle, which was enhanced by monocyte administration. Again, CD11b$^+$ cells retrieved from the VEGF^{ON} livers, representing VEGF-educated monocytes, enhanced angiogenesis significantly better than CD11b$^+$ cells retrieved from WT P-LAP-tTA$^+$/tet-VEGF^{OFF} livers (Fig. 4 d).

The hind limb ischemia model is particularly suitable for studying arteriogenesis

Here, arteriogenic responses in the region immediately downstream of the ligation resulting in increased diameter of preexisting collateral vessels are made evident by angiography. As shown in Fig. 4 (e and f), at 14 d after occlusion control PBS-injected animals still showed a marked perfusion deficit, and systemic administration of monocytes isolated from the P-LAP-tTA$^+$/tet-VEGF^{OFF} liver demonstrated a modest improvement on the angiogenic score. In contrast, VEGF-educated monocytes induced collateral development to the extent that normal perfusion was fully restored. The latter result highlights the key role of VEGF in enhancing the arteriogenic function of recruited monocytes. Intriguingly, the beneficial effect of VEGF-educated monocytes on collateral growth was observed at a time point where grafted, preeducated monocytes should have already been eliminated when considering the fact that they are short-lived. A possible explanation is that the grafted preeducated monocytes imitate a cascade of events that may proceed even in their absence, including the possibility of subsequent recruitment of other cell types.

Mechanistic aspects of VEGF-induced reprogramming of recruited monocytes

VEGF functions in relation to nonendothelial cells could, in principle, be a direct effect mediated by VEGF receptors expressed by these nonendothelial cells or an indirect effect mediated by angiocrine factors elaborated by the VEGF-activated endothelium, with several precedents existing for both cases. Because the only VEGF receptor known to be expressed by monocytes is VEGFR1 (Sawano et al., 2001), we addressed the possibility of a direct effect through precluding VEGFR1 signaling in recruited monocytes. To this end, we performed adoptive transfer experiments using mutant VEGFR1 monocytes in which the native VEGFR1 has been replaced with a tyrosine kinase–dead VEGFR1 (Hiratsuka et al., 1998). To make the comparison with WT monocyte as accurate as possible, we adoptively transferred a 1:1 mixture of differentially tagged WT and VEGFR1 mutant monocytes and compared their trafficking into the VEGF-induced liver. Results revealed no impediment in the recruitment process, as indicated by a comparable number of monocytes recruited to the VEGF-induced liver (Fig. 5 a). To determine whether recruited monocytes lacking a functional VEGFR1 are capable of undergoing VEGF-instructed reprogramming, we followed changes in surfaces markers signifying the education process after their adoptive transfer exemplified by down-regulated Ly6C and up-regulated CD36 surface expression. As shown in Fig. 5 b, the same changes undergone by WT monocytes (Fig. 6, b and d, down-regulated Ly6C and up-regulated CD36, respectively) also took place in VEGFR1 mutant monocytes, and again only in the VEGF-induced liver. These results suggest that the sole VEGF receptor expressed by monocytes is dispensable for the education process, thus favoring an indirect VEGF mechanism.

To determine whether CCR2 or CX_3CR1, the main chemotactic receptors expressed on VEGF-recruited monocytes are essential for the recruitment process, we adoptively transferred monocytes nullified for these chemokine receptors. In brief, CX_3CR1 KO monocytes or CCR2 KO monocytes were adoptively transferred into the circulation of the VEGF-induced mice at a 1:1 mixture with labeled WT cells, and their numbers within the liver were compared with that of WT monocytes. In the case of CX_3CR1 KO monocytes, no difference in the number of recruited cells was observed, thus arguing against an essential mediating role of CX_3CR1 in VEGF-induced recruitment. In the case of CCR2 KO monocytes, the number of recruited cells was reduced to about one third of that of WT monocytes. However, this was mirrored in a similarly reduced number of transferred monocytes detected in the circulation 3 d after transfer, thus precluding assigning a mediating role for CCR2 in VEGF-induced recruitment (Fig. 5 a).

To gain further molecular insights on VEGF-induced reprogramming, we compared gene expression signatures of naive and educated monocytes using high-throughput transcriptome analysis. We again resorted to adoptive transfers of labeled monocytes, followed by their retrieval from the liver. To further refine the analysis, we designed a novel tandem-transfer strategy where fluorescently labeled monocytes were first introduced into the circulation of mice in which VEGF had been switched ON 14 d earlier, followed by a second monocyte transfer (this time with a different label) 2 d later. Retrieval of monocytes 1 d later, and sorting according to the two labels indicative of the time spent in the VEGF-induced organ, allowed us to follow the dynamics of post-recruitment changes in gene expression (Fig. 6 a). Validating the suitability of this experimental strategy for sorting newly arrived from

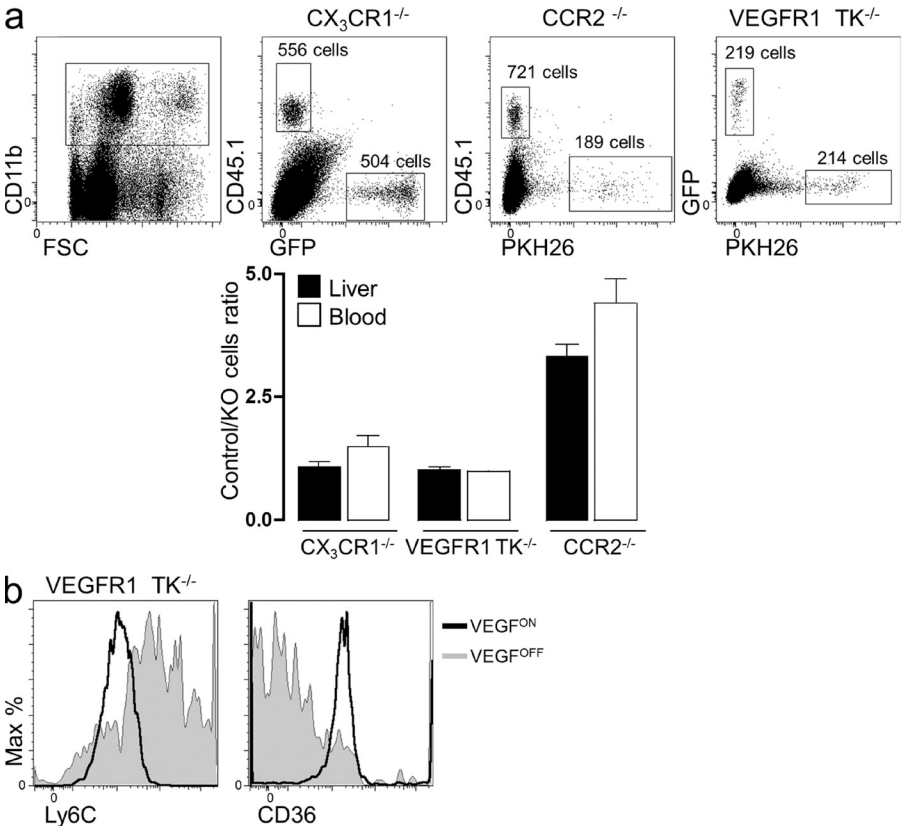

Figure 5. VEGF-instructed recruitment of monocytes nullified for VEGFR1, CX_3CR1, and CCR2. (a) The respective mutant monocytes were isolated, mixed with WT monocytes at a 1:1 ratio, and adoptively transferred into mice with an ongoing VEGF switch ($VEGF^{ON}$) as described above. Monocytes were subsequently retrieved 3 d after transfer, and the number of recruited monocytes of each genotype was determined by flow cytometry. To aid distinction between recruited WT and mutant monocytes, the following monocyte mixtures were transferred: $CX_3CR1^{+/gfp}$: (PKH26)-VEGFR1$TK^{-/-}$, CD45.1: (PKH26)-$CCR2^{-/-}$, and CD45.1: $CX_3CR1^{gfp/gfp}$. Representative of $n = 3$ independent mice per group. (b) VEGFR1$TK^{-/-}$ monocytes were adoptively transferred into $VEGF^{ON}$ and $VEGF^{OFF}$ mice as described above. 3 d after transfer, cells were retrieved and analyzed for their expression of the membrane markers Ly6C and CD36. Representative of $n = 3$ independent mice per group.

veteran monocytes, the first cohort (carrying the PKH26 red label) were found to have not yet converted to the $Ly6C^{lo}$ phenotype, whereas the latter cohort (carrying the CSFE green label) had already done so (Fig. 6 b). A principle component analysis (PCA) comparing the input naive monocytes with monocytes retrieved at 24 h or at 72 h has provided a visual illustration that this experimental design, indeed, uncouples changes taking place in the circulation or associated with extravasion and entry from changes occurring in the target organ, with the latter reflecting progressive education (Fig. 6 c). Correspondingly, out the several hundred genes up-regulated in the target organ, we focused on those, which are further up-regulated in recruited monocytes between the first and third day of residence in the VEGF-induced liver, i.e., the differential of newly arrived and veteran monocytes (Fig. 6 c). Some representative genes up-regulated between the first and third day from arrival are highlighted in the figure and the 24 most up- or down-regulated genes during this time interval are listed in Table S1. For some genes encoding surface markers like CD9 and CD36 this was also corroborated by FACS analysis of the respective genes (Fig. 6 d).

Notably, $Ly6C^{hi}$ monocytes convert by default with time into $Ly6C^{lo}$ monocytes (Varol et al., 2007; Yona et al., 2012). To discriminate the expression changes associated with this spontaneous conversion from the ones imprinted by the VEGF environment, we performed a differential of differentials by comparing the changes observed between newly arrived ($Ly6C^{hi}$) from veteran ($Ly6C^{lo}$) monocytes, with the reported changes between circulating $Ly6C^{hi}$ and $Ly6C^{lo}$ monocytes (Ingersoll et al., 2010). We found 80 genes to overlap (Fig. 6 c), 58 of which were commonly up-regulated in both $Ly6C^{lo}$ subsets and 22 of which were specifically up-regulated in VEGF educated monocytes and down-regulated in $Ly6C^{lo}$ circulating monocytes.

Reasoning that there are different forms of monocyte education dictated by different educators and culminating in a different phenotypic outcome and to show the uniqueness of VEGF-instructed education, we wished to compare our case with an unrelated process of monocyte reprogramming taking place in the same organ. Of the available datasets, most relevant was a very recently published dataset analyzing adoptively transferred $Ly6C^{hi}$ monocytes recruited to the liver in a murine liver fibrosis model (Ramachandran et al., 2012). This particular comparison was chosen because both systems interrogate the same subset of adoptively transferred monocytes, recruited to the same organ where they change their phenotype from $Ly6C^{hi}$ to $Ly6C^{lo}$. They were retrieved for analysis at a similar time frame (24–72 h) and analyzed using the same gene arrays. Yet, the education process appears to be remarkably different, with only a small fraction (one sixth) of recorded changes taking place between day 1 and 3 in our system. This fraction occurred with changes taking place at the same interval in the other system, with both showing a phenotype outside the M1/M2 classification (Fig. 6 e). Moreover, although both cases were dominated by changes in the cytokines and receptors and extracellular matrix categories,

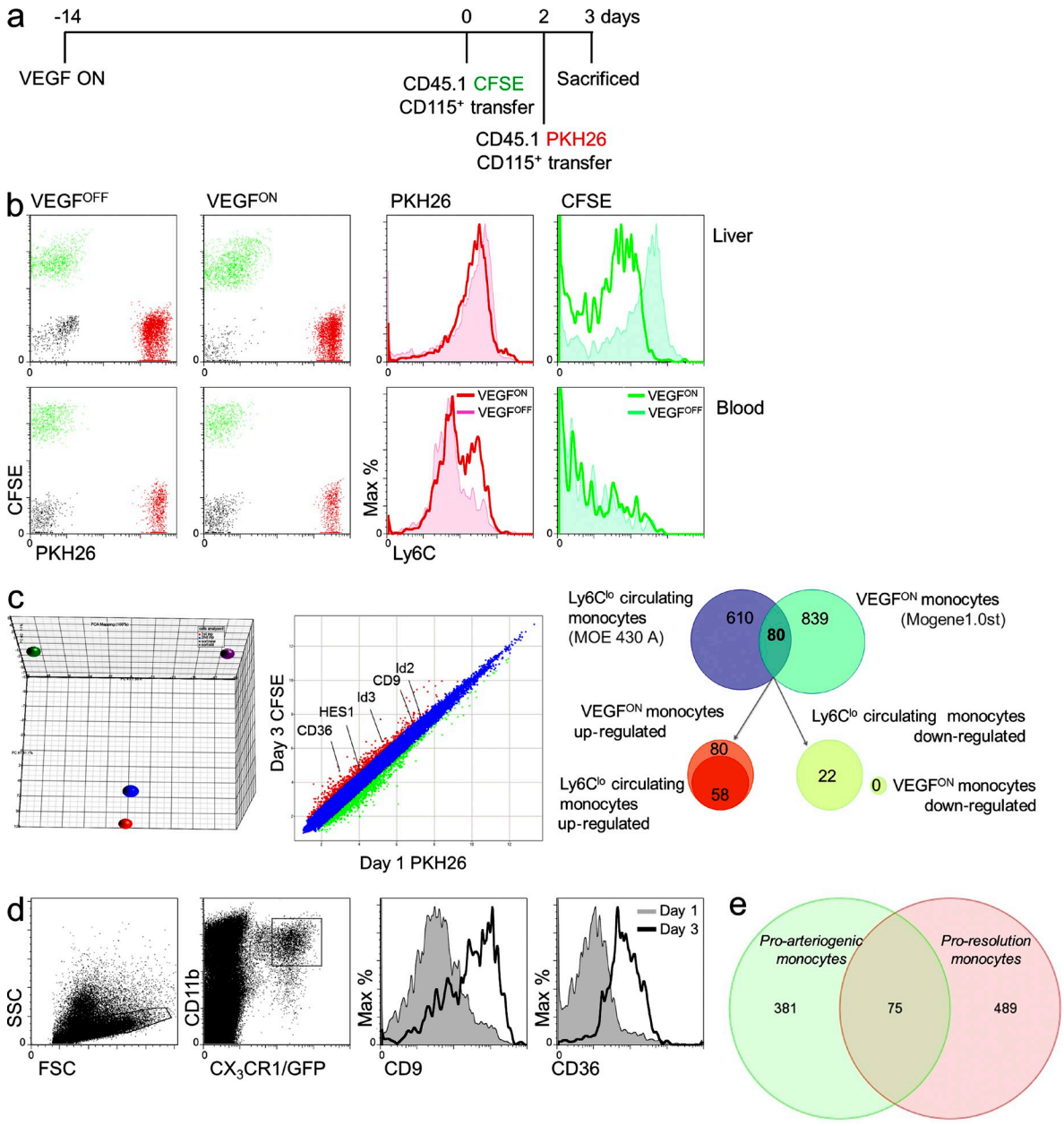

Figure 6. Transcriptomic changes associated with VEGF-instructed monocyte reprogramming. (a) Scheme of the experimental design: to follow the changes occurring in the monocyte-derived populations subsequent to their arrival to the VEGF-induced liver, tandem transfer strategy was designed. In this experiment ,the transfer of CD45.1$^+$ BM monocytes labeled with CFSE (on day 0) was followed by transfer of CD45.1$^+$ BM monocytes labeled with PKH26 (on day 2), and retrieval for analysis occurred a day later (on day 3). (b) Mice were killed on day 3, and the two populations of grafted cells were separated from both blood and liver (left). Analysis of Ly6C expression (right). Representative of $n = 4$ mice per group, performed twice. (c, left) PCA of naive and VEGF-educated monocytes. PCA analysis of adoptively transferred monocytes comparing input (naive) monocytes (red and blue circles of CFSE- and PKH26-tagged monocytes, respectively) and educated monocytes (purple and green circles representing monocytes retrieved at 72 and 24 h after transfer, respectively. Comparative transcriptomic analysis of CSFE-labeled (veteran/educated) and PKH26-labeled (newly arrived) monocytes highlights the down-regulation of genes between day 1 and 3 of residence in the liver and exposure to the VEGF milieu. (c, right) Differential of the differential. Analysis of the differential between newly arrived ($Ly6C_{hi}$) and veteran/educated ($Ly6C_{lo}$) monocytes and the differential between $Ly6C^h$i and $Ly6C_{lo}$ circulating monocytes demonstrated an overlap of only 80 genes. 58 of these genes were up-regulated in both $Ly6C^{lo}$ subsets, whereas 22 genes were specifically up-regulated in the $Ly6C^{lo}$ $VEGF^{ON}$ veteran monocytes. Cells were isolated as described in a and b and pooled from seven mice. Experiment was performed in duplicate. (d) Verification of transcriptome analysis, BM CD115$^+$ monocytes were isolated from $CX_3CR1^{GFP/+}$ donors and transferred to $VEGF^{ON}$ mice. 1 and 3 d after cell transfer, grafted cells from the livers of recipient mice were analyzed for their expression of CD9 and CD36. Representative of $n = 3$ mice per group per time point. (e) A Venn diagram comparing the transcriptomes of adoptively transferred $Ly6C^{hi}$ monocytes retrieved from VEGF-induced liver (green) or from a fibrotic liver (pink). Genes subjected for this comparison were all those showing >1.5-fold change (up or down) between 24 and 72 h from transfer. Data on fibrosis proresolution monocytes were obtained from Ramachandran et al. (2012).

different genes within these categories showed altered expression (unpublished data).

In the genes up- or down-regulated as a result of VEGF-instructed reprogramming, we found genes associated with the pathways of transendothelial migration, cell adhesion molecules, ECM-ECM receptor interactions, and cytokine-cytokine receptor interactions (Fig. 7). Genes specific to VEGF-induced monocyte differentiation included MMP8, a matrix metalloproteinase capable of cleaving native fibrillar collagens, and Timp2, a regulator of directed angiogenesis.

Other notable examples for the latter category were genes in the Notch pathway and Id genes and their respective targets (Fig. 7). The Notch pathway is of interest because of an increasing body of evidence for its involvement in various aspects of neovascularization (Phng and Gerhardt, 2009), as well as in the process of macrophage polarization (unpublished data). Id gene expression patterns in BM-derived cells are of particular interest because of their essential role in tumor angiogenesis (Lyden et al., 2001). Notably, Id2 expression was specifically induced in monocytes recruited to the VEGF-induced liver, but not in monocytes that had homed to the naive liver, and was further up-regulated within the organ between day 1 and 3 (Fig. 6 c and not depicted). This unique system provides a suitable experimental platform to examine candidate mediators of VEGF-induced reprogramming of recruited monocytes.

DISCUSSION

This study addressed two fundamental open questions regarding cell-assisted adult neovascularization. First, what is the origin of monocytes recruited to sites of ongoing neovascularization and functioning therein as paracrine accessories? Specifically, is there a specialized subset of proangiogenic, BM-derived monocytes? The study clearly rules out this possibility by showing that VEGF-recruited monocytes are derived from the pool of circulating Ly6C^{hi} monocytes, which are also known to serve as precursors for descendant macrophages and inflammatory dendritic cells (Yona and Jung, 2010). However, the extravasated monocytes were found to exert their proangiogenic function as short-lived monocytes without differentiating into persistent macrophages. Second, is the proangiogenic activity of recruited monocytes an inherent or acquired property? The study clearly shows that functional performance of recruited monocytes is greatly improved via a process of VEGF-instructed reprogramming taking place at the target tissue.

Together, these findings uncover a mechanism for monocyte-assisted neovascularization making use of the abundant pool of circulating standard monocytes and exploiting their inherent plasticity for their on-site conversion into effective paracrine accessory cells. This rather simple mechanism is significantly more cost-effective than maintaining a subset of specialized monocytes ready to be called on demand. Our findings that recruited monocytes are reprogrammed within three days from arrival at the target organ and continue to stay there only for few days longer as nonreplicating monocytes, suggest that a constant influx with new monocytes is required for a continuous, efficient neovascularization. This also provides a simple way to terminate the angiogenic response and clear the tissue from infiltrated monocytes shortly after terminating the VEGF signal.

Myeloid cell education has been argued in different settings, including in the context of tumor-infiltrating macrophages (Qian and Pollard, 2010). However, considering the many cell types populating the tumor microenvironment already at the earliest time point analyzed, it has been impossible to exclude other mechanisms accounting for the apparent heterogeneity. For example, selective recruitment of either Ly6C^{hi} or Ly6C^{lo} monocytes mediated by uncharacterized acute triggers has been demonstrated for the healing myocardium (Nahrendorf et al., 2007), whereas a phenotypic switch from Ly6C^{hi} to Ly6C^{lo} monocytes, likely mediated by phagocytosed debris ,was described for skeletal muscle cell regeneration (Arnold et al., 2007). In the present study, selective recruitment of even a minor population was ruled out by demonstrating phenotypic conversion of a preselected homogenous population of Ly6C^{hi} monocytes. Another possible explanation for the emerging differences between grafted and retrieved monocytes, namely, preferential on-site expansion of a minor subpopulation, seemed unlikely in view of the nonproliferative nature of monocytes (van Furth et al., 1979) and the relatively short time interval from transfer to analysis. This was, nevertheless, corroborated using CSFE label retention experiments indicating a lack of appreciable monocyte proliferation. This study, we believe, is the first to follow active monocyte reprogramming in vivo in settings where both the identity of the educator and the functional outcome of education are clearly defined. To this end, we took advantage of the unique features of our experimental system, including the ability to recruit at will tagged monocytes to a naive organ and subsequently retrieve them, and the ability to analyze not only endogenously recruited monocytes but also adoptively transferred monocytes. Sequential transfer of differentially labeled monocytes, in particular, enabled us to follow the ongoing reprogramming independently of other processes, culminating in monocyte diversification.

Generally, myeloid cell education may lead to acquisition of different specialized functions determined by the nature of the educator. Here, we focused on VEGF as monocyte educator, reasoning that the monocytes recruited by VEGF are not angiogenic professional cells, and thus VEGF may act to enhance their proangiogenic capabilities.

Because we used a clean genetic VEGF switch, all phenotypic changes are, by definition, downstream of VEGF activation. Interestingly, the VEGFR1-selective VEGF homologue PLGF was previously shown not only to be required for macrophage infiltration in atherogenesis (Khurana et al., 2005) but also to possess proarteriogenic activity via a monocyte-mediated mechanism involving changes in integrin surface expression (Pipp et al., 2003). It is thus likely that PLGF is also capable of reprogramming recruited monocytes, and it remains to be determined if and how VEGF- and PLGF-instructed monocyte education are interrelated.

a

Pathway	Impact factor	p-value
Hematopietic cell lineage	13.27	1.73E-06
Cell adhesion molecules (CAMS)	9.31	9.01E-05
Antigen processing presentation	8.57	1.90E-04
Cytokine-cytokine receptor interaction	7.43	5.93E-04
Leukocyte transendothelial migration	3.65	0.02
ECM-receptor interaction	3.15	0.04

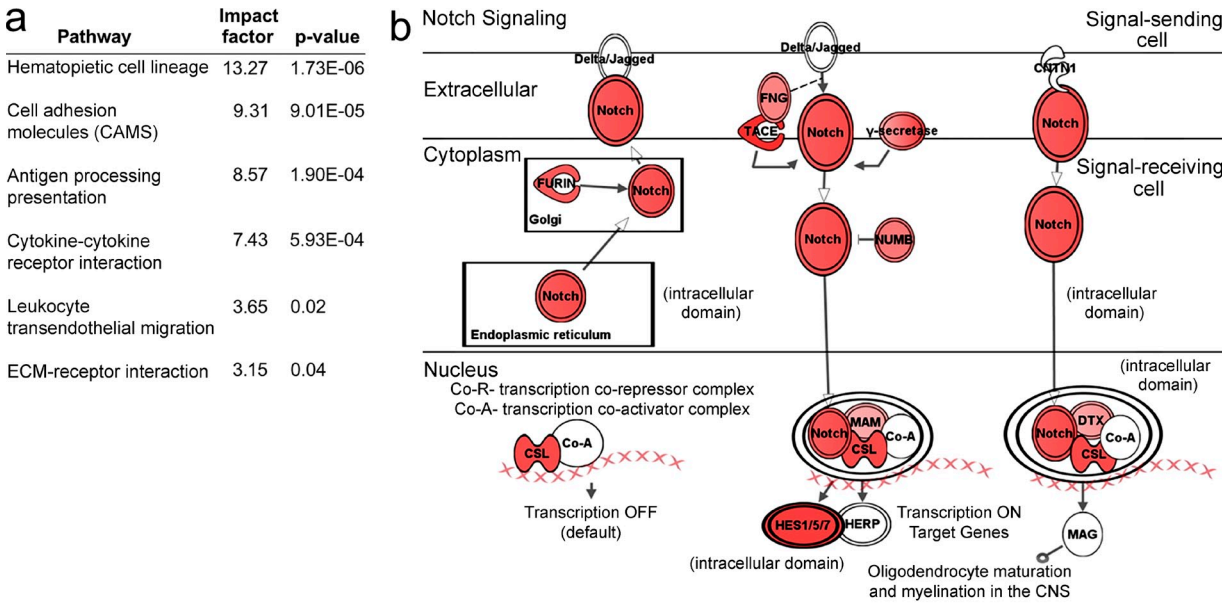

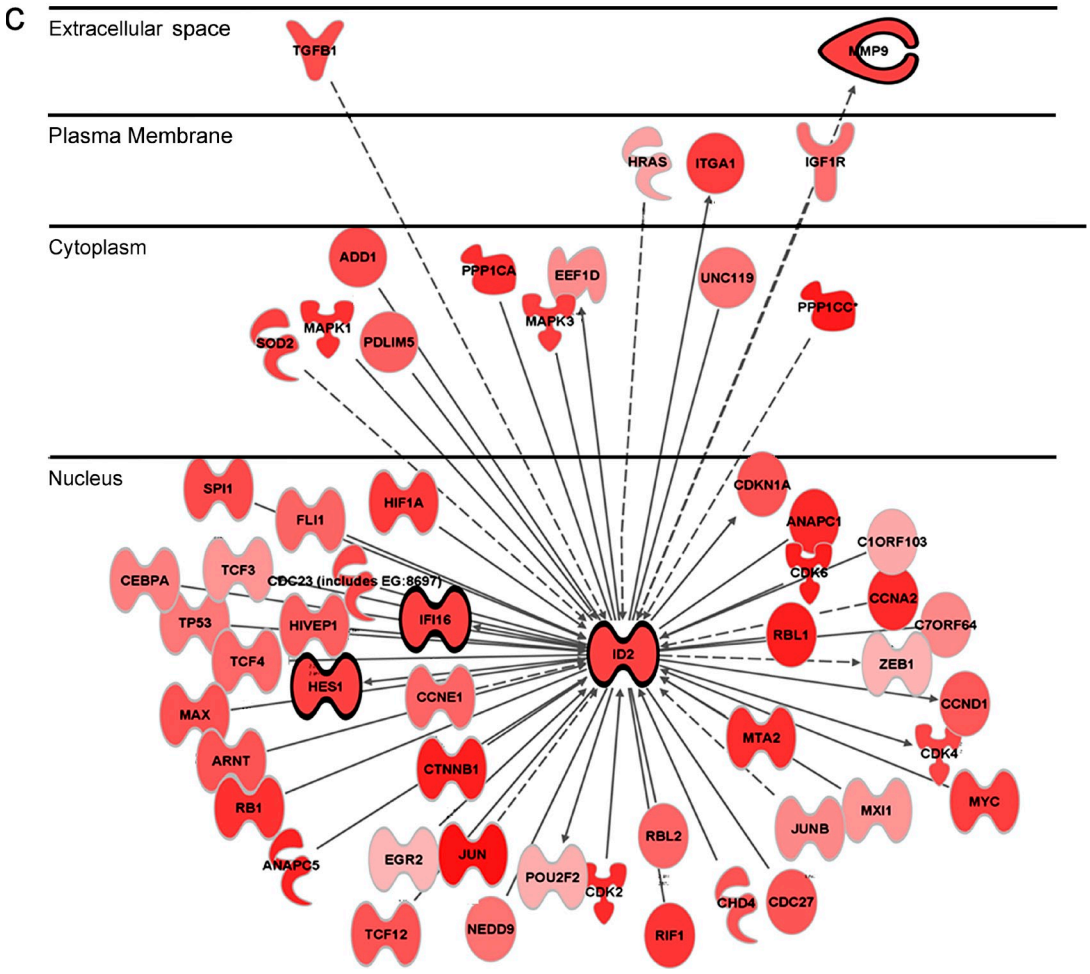

Figure 7. Transcriptomic changes of adoptively transferred monocytes upon VEGF–instructed reprogramming. Transcriptomes of CSFE-labeled monocytes and PKH26-labeled monocytes obtained as described in Fig. 6 a using the tandem transfer strategy and representing relatively old and new arrivals to the liver, respectively, were compared. (a) GO analysis highlighting some pathways enriched in monocytes retrieved at day 3 relative to monocytes retrieved at day 1. (b and c) Inginuity software-aided analysis of components of the Notch and Id pathways, respectively. Genes surrounded by light ring are genes that were up-regulated between transferred cells and retrieved cells. Genes surrounded by dark ring are genes that were up-regulated between day 1 and day 3. The darker the red the more pronounced the up-regulation.

It is not known whether VEGF acts directly on recruited monocytes or whether the effects are mediated by other VEGF-induced factors, including by factors released by the VEGF-activated endothelium. A direct VEGF effect is feasible considering that recruited monocytes express VEGFR1. Yet, we show that monocytes incapable of direct VEGF signaling are similarly reprogrammed by VEGF within the target organ, thus supporting an indirect effect.

Adult neovascularization promoted by VEGF, including tumor neovascularization, necessitates not only inducing sprouting angiogenesis, which results in the formation of capillaries, but also the formation of larger vessels. We propose that the principle function of VEGF-recruited monocytes is, in fact, to support the arterialization process. This proposition is supported by the finding that upon inhibition of monocyte recruitment, the process most affected is EC proliferation in the context of existing larger vessels, a process leading to their circumferential growth, and by the finding that after VEGF education these monocytes strongly facilitate formation of large conduits in a surrogate collateralization system (Fig. 4, e and f). The key role of monocytes in the process of collateralization triggered by vessel occlusion and increased shear stress in vessels to which flow has been diverted has been demonstrated in the seminal work of Schaper et al. (1976). Additional work supports a scenario where an increase in shear stress and resultant NO production induces VEGF which, in turn, induces monocyte chemoattractants (Matthews et al., 2003; Pipp et al., 2003; Schaper, 2009). Our earlier study showing that VEGF acts to recruit monocytes independently of hemodynamic factors (Grunewald et al., 2006), in conjunction with the novel findings reported here that VEGF acts to enhance arteriogenic capabilities of recruited monocytes, strongly suggest that VEGF-educated monocytes are also key players in arterialization in the context of de novo adult arterialization. Considering that on its own VEGF is a poor EC mitogen, it is likely that VEGF reprogramming toward a proarteriogenic phenotype includes up-regulation of secreted EC mitogens. Previous studies using endothelial/monocyte co-cultures have shown that the proproliferative effect of monocytes on endothelial cells requires cell–cell contact and is, at least in part, mediated by Met and ERK activation (Schubert et al., 2008).

Molecular mediators of VEGF-instructed monocyte education should be separated in two different categories, namely, the factors mediating monocyte reprogramming proper and the pro-angiogenic/arteriogenic factors induced as a consequence of reprogramming. With regard to the former, the oxygen sensor PHD2 has been shown to play a role in macrophage skewing toward a proarteriogenic phenotype (Takeda et al., 2011), and with respect to the latter, previous studies have highlighted the roles played by metaloproteases (Jin et al., 2006). Further work is clearly required, however, to elucidate the molecular mediators in both categories.

VEGF-induced reprogramming may also include a component that actively inhibits the differentiation of recruited monocytes into macrophages. Id genes, known to function as inhibitors of differentiation and shown here to be induced by VEGF in recruited monocytes are attractive candidates to fulfill this function.

Finally, findings reported here provide new insights pertinent to contemplated proangiogenic therapies, in general, and to therapeutic modalities based on administration of BM cells, in particular. Clinical trials using autologous BM transplantation to the infarcted myocardium were initially based on the presumed contribution of EPCs and, accordingly, used ex vivo manipulations aiming at EPC enrichment (Kawamoto et al., 2001). Our findings suggest that the beneficial effect of grafted BM-derived cells might rather be attributed to monocytes with further improvement by VEGF, hinting at new approaches for enhancing the utility of BM-derived cells in this direction.

MATERIALS AND METHODS

Transgenic mice. This study involved the use of the following 6–8-wk-old mice: WT C57BL/6 mice, congenic CD45.1 mice, nude or heterozygote or homozygote mutant $CX_3CR1^{GFP/+}$ mice (Jung et al., 2000), $CCR2^{-/-}$ mice (Boring et al., 1997), and $VEGFR1TK^{-/-}$ mice (Hiratsuka et al., 1998). For liver-specific VEGF induction, P-LAP mice, in which tTA expression is driven by a C/EBPb (CCAAT/enhancer binding protein b, in the liver; Kistner et al., 1996), were crossed with the responder tet-VEGF164 transgenic mice (Dor et al., 2002), these mice were termed P-LAP-tTA^+/tet-$VEGF^+$. Additionally, P-LAP-tTA^+/tet-$VEGF^+$ was further crossed with the $CX_3CR1^{GFP/+}$ mouse. VEGF was induced in mature 6–8-wk-old mice after the withdrawal of tetracycline from the drinking water ($VEGF^{ON}$), blood samples were monitored for the efficiency of VEGF induction (circulating VEGF levels of >650 pg/ml compared with <40 pg/ml detected in $VEGF^{OFF}$ mice), using a standard VEGF ELISA assay (R&D Systems). All mice studied were on C57BL/6 background, maintained under specific pathogen–free conditions, and handled under protocols approved by the Weizmann Institute Animal Care Committee and Hadassah Medical School (MD 09–11916-2), in accordance with international guidelines.

Cell isolations and analysis isolation of circulating monocytes. Mice were anesthetized and peripheral blood was collected via cardiac puncture and subjected to Ficoll density gradient (GE Healthcare) to retrieve the mononuclear fraction (Yona et al., 2010).

Isolation of liver monocytes. Mice were perfused with 50 ml of cold PBS and livers were excised. Livers were subsequently digested with 1 mg/ml collagenase D (Roche; 1 h at 37°C), and filtered through 80 μM wire mesh. Density centrifugation enriched the liver suspension for mononuclear phagocytes. In brief, the resulting pellet was resuspended in 40% Percoll (Sigma-Aldrich) layered on 80% Percoll before density centrifugation (1,000 *g* for 15 min at 20°C with low acceleration and no brake), enriched cells were isolated from the interphase, and erythrocytes were removed by ACK lysis. Cells were resuspended in PBS supplemented with 2 mM EDTA, 0.05% sodium azide, and 2% FCS. Fluorochrome-labeled monoclonal antibodies purchased from BioLegend (CD45.1, CD9, CD36, GR1 and Ly6C), eBioscience (CD115, CD11b and CD11c), R&D Systems (CD64), ABD Serotec (F4/80), or Invitrogen (Annexin V kit and Sytox) and used according to the manufacturer's instructions. Cells were analyzed with a FACSCalibur or LSR Fortessa flow cytometer (BD) and analyzed offline using FlowJo software (Tree Star).

Cell transfer for BM monocyte transfer. Cells were harvested from the femora and tibiae and mononuclear cells enriched by Ficoll density gradient centrifugation. The mononuclear fraction was washed in PBS supplemented with 2 mM EDTA and 2% FCS and cells were incubated with anti–CD115-biotin (eBioscience), followed by incubation with streptavidin-conjugated

MACS beads (Miltenyi Biotec). Cells were then magnetically separated, according to manufacturer's instructions. $CD115^+$ fraction was collected and 1.5×10^6 cells injected i.v. to recipient mice. In particular experiments the cells were further immunostained with CD115 and Ly6C; specific populations were then purified by high-speed cell sorting using a FACS Aria (BD). For the tandem transfer study, congenic CD45.1 monocytes were labeled with the intracellular fluorescent dye CFSE (Invitrogen) or PKH26 (Sigma-Aldrich) according to the manufactures instructions before their transfer.

Array processing. All experiments were performed using Affymetrix Mouse Gene 1.0st oligonucleotide arrays, in accordance to the manufacturer's instructions. Total RNA from each sample was used to prepare biotinylated target DNA. In brief, 100 ng of total RNA was used to generate first-strand cDNA by using a T7-random hexamers primer. After second-strand synthesis, in vitro transcription was performed. The resulting cRNA was then used for a second cycle of first-strand cDNA by using a T7-random hexamers primer with UTP, resulting in SS DNA used for fragmentation and terminal labeling. The target cDNA generated from each sample was processed using an Affymetrix GeneChip Instrument System. Spike controls were added to a 5.5-µg fragment of cDNA before overnight hybridization. Arrays were then washed and stained with streptavidin-phycoerythrin, before being scanned on an Affymetrix GeneChip scanner. The quality and concentration of starting RNA was confirmed using an agarose gel and Bioanalyzer (Agilent). The signals derived from the array were assessed using quality assessment metrics.

Data analysis. Gene level RMA sketch algorithm (Affymetrix Expression Console and Partek Genomics Suite 6.2) was used for crude data generation. A comparison between samples was performed using various algorithms, including clustering and fold change calculations. Genes were filtered and analyzed using unsupervised hierarchical cluster analysis (Spotfire DecisionSite for Functional Genomics).

Aortic ring sprouting assay. Thoracic aortas were dissected from 8–10-wk-old male mice. The adventitia was removed and 0.5 mm "rings" were embedded in collagen as described by (Licht et al., 2003). The collagen was then overlaid with either medium alone (BIO-MPM-1) or a medium supplemented with 10 ng/ml VEGF or conditioned medium from $CD11b^+$ cells isolated from either $VEGF^{OFF}$ or $VEGF^{ON}$ livers, the plates were incubated at 37°C in a humidified 5% CO_2 atmosphere, and medium was replaced every 48 h. After a 7-d incubation, the rings were fixed in 4% formaldehyde for 24 h, followed by staining with crystal violet (0.02%). Micrographs of representative rings taken by morphometric analysis of sprouting were performed on four rings manually using ImageJ (National Institutes of Health) software (Nissanov et al., 1995).

Hind limb ischemia and neovascularization. Nude mice underwent surgical ligature at the proximal section of the right femoral artery, as described previously (Zouggari et al., 2009). In brief, 10^5 $CD11b^+$ cells isolated from livers were injected retroorbitally 8 h after femoral artery ligation. 14 d later, postischemic neovascularization was evaluated by microangiography and capillary density analysis.

Immunohistochemistry. After 50-ml perfusion of cold PBS, livers were excised, fixed for 3 h in 4% paraformaldehyde, equilibrated for 36 h in 30% sucrose in PBS-T, imbedded in OCT, and frozen at −80°C. 7-µm-thick cryostatic sections were post-fixed with cold methanol, blocked with CAS block, and stained using anti-CD31 and vWF (Dako) as primary antibodies overnight. Alexa Fluor 555 anti–rabbit antibody (Invitrogen) was used as secondary antibody for 2 h. Slides were finally mounted in fluorescent mounting medium supplemented with DAPI (2 µg/ml; Sigma-Aldrich). For Ki67 immunostaining, 5-µm paraffin sections were used, antigen was retrieved by microwaving at 92°C in citrate buffer (pH 6; Zymed Laboratories Inc.) for 20 min, polyclonal Ki67 (Thermo Fisher Scientific) was used as a primary antibody, and chromogenic detection was performed using ImmPRESS UNIVERSAL (Vector Laboratories). Analysis by confocal laser scanning microscopy was performed using a Carl Zeiss LSM510 microscope. Representative pictures were collected and analyzed using MetaMorph software.

Cell proliferation. Assay labeling of proliferating cells was performed by an i.p. injection of BrdU, 3 h before sacrificing the animal and visualizing $BrdU^+$ cells in paraffin sections using anti-BrdU antibodies (BrdU detection kit; GE Healthcare).

Statistics. In all cases data are expressed as mean ± SEM. Statistical analysis performed between two datasets by Student's *t* test, whereas analysis of three or more datasets was performed using one-way ANOVA, followed by Bonferroni test. A p-value <0.05 was accepted to reject the null hypothesis.

Online supplemental material. Fig. S1 shows flow cytometry analysis of GFP-positive blood monocytes. Table S1 is a list of genes exhibiting the highest change (log) in expression comparing monocytes retrieved at 72 h after transfer. Online supplemental material is available at http://www.jem.org/cgi/content/full/jem.20120690/DC1.

We thank Prof. Gideon Rechavi and Jasmine Jacob-Hirsch for producing the microarray data and Dr. Yoav Smith for the bioinformatics analysis.

This work was supported by a long-term FEBS Fellowship (S. Yona) the Israeli Science Foundation (S. Jung and E. Keshet), the German-Israel Foundation, and a Israel Cancer Research fund professorship award (E. Keshet).

The authors declare no competing financial interests.

Submitted: 29 March 2012
Accepted: 26 September 2013

REFERENCES

Arnold, L., A. Henry, F. Poron, Y. Baba-Amer, N. van Rooijen, A. Plonquet, R.K. Gherardi, and B. Chazaud. 2007. Inflammatory monocytes recruited after skeletal muscle injury switch into antiinflammatory macrophages to support myogenesis. *J. Exp. Med.* 204:1057–1069. http://dx.doi.org/10.1084/jem.20070075

Boring, L., J. Gosling, S.W. Chensue, S.L. Kunkel, R.V. Farese Jr., H.E. Broxmeyer, and I.F. Charo. 1997. Impaired monocyte migration and reduced type 1 (Th1) cytokine responses in C-C chemokine receptor 2 knockout mice. *J. Clin. Invest.* 100:2552–2561. http://dx.doi.org/10.1172/JCI119798

Cai, W., and W. Schaper. 2008. Mechanisms of arteriogenesis. *Acta Biochim. Biophys. Sin. (Shanghai).* 40:681–692.

De Palma, M., M.A. Venneri, C. Roca, and L. Naldini. 2003. Targeting exogenous genes to tumor angiogenesis by transplantation of genetically modified hematopoietic stem cells. *Nat. Med.* 9:789–795. http://dx.doi.org/10.1038/nm871

De Palma, M., M.A. Venneri, R. Galli, L. Sergi Sergi, L.S. Politi, M. Sampaolesi, and L. Naldini. 2005. Tie2 identifies a hematopoietic lineage of proangiogenic monocytes required for tumor vessel formation and a mesenchymal population of pericyte progenitors. *Cancer Cell.* 8:211–226. http://dx.doi.org/10.1016/j.ccr.2005.08.002

Dor, Y., V. Djonov, R. Abramovitch, A. Itin, G.I. Fishman, P. Carmeliet, G. Goelman, and E. Keshet. 2002. Conditional switching of VEGF provides new insights into adult neovascularization and pro-angiogenic therapy. *EMBO J.* 21:1939–1947. http://dx.doi.org/10.1093/emboj/21.8.1939

Geissmann, F., S. Jung, and D.R. Littman. 2003. Blood monocytes consist of two principal subsets with distinct migratory properties. *Immunity.* 19:71–82. http://dx.doi.org/10.1016/S1074-7613(03)00174-2

Grunewald, M., I. Avraham, Y. Dor, E. Bachar-Lustig, A. Itin, S. Jung, S. Chimenti, L. Landsman, R. Abramovitch, and E. Keshet. 2006. VEGF-induced adult neovascularization: recruitment, retention, and role of accessory cells. *Cell.* 124:175–189. http://dx.doi.org/10.1016/j.cell.2005.10.036

Hiratsuka, S., O. Minowa, J. Kuno, T. Noda, and M. Shibuya. 1998. Flt-1 lacking the tyrosine kinase domain is sufficient for normal development

and angiogenesis in mice. *Proc. Natl. Acad. Sci. USA*. 95:9349–9354. http://dx.doi.org/10.1073/pnas.95.16.9349

Ingersoll, M.A., R. Spanbroek, C. Lottaz, E.L. Gautier, M. Frankenberger, R. Hoffmann, R. Lang, M. Haniffa, M. Collin, F. Tacke, et al. 2010. Comparison of gene expression profiles between human and mouse monocyte subsets. *Blood*. 115:e10–e19. http://dx.doi.org/10.1182/blood-2009-07-235028

Jin, D.K., K. Shido, H.G. Kopp, I. Petit, S.V. Shmelkov, L.M. Young, A.T. Hooper, H. Amano, S.T. Avecilla, B. Heissig, et al. 2006. Cytokine-mediated deployment of SDF-1 induces revascularization through recruitment of CXCR4+ hemangiocytes. *Nat. Med.* 12:557–567. http://dx.doi.org/10.1038/nm1400

Jung, S., J. Aliberti, P. Graemmel, M.J. Sunshine, G.W. Kreutzberg, A. Sher, and D.R. Littman. 2000. Analysis of fractalkine receptor CX(3)CR1 function by targeted deletion and green fluorescent protein reporter gene insertion. *Mol. Cell. Biol.* 20:4106–4114. http://dx.doi.org/10.1128/MCB.20.11.4106-4114.2000

Kawamoto, A., H.C. Gwon, H. Iwaguro, J.I. Yamaguchi, S. Uchida, H. Masuda, M. Silver, H. Ma, M. Kearney, J.M. Isner, and T. Asahara. 2001. Therapeutic potential of ex vivo expanded endothelial progenitor cells for myocardial ischemia. *Circulation*. 103:634–637. http://dx.doi.org/10.1161/01.CIR.103.5.634

Khurana, R., L. Moons, S. Shafi, A. Luttun, D. Collen, J.F. Martin, P. Carmeliet, and I.C. Zachary. 2005. Placental growth factor promotes atherosclerotic intimal thickening and macrophage accumulation. *Circulation*. 111:2828–2836. http://dx.doi.org/10.1161/CIRCULATIONAHA.104.495887

Kistner, A., M. Gossen, F. Zimmermann, J. Jerecic, C. Ullmer, H. Lübbert, and H. Bujard. 1996. Doxycycline-mediated quantitative and tissue-specific control of gene expression in transgenic mice. *Proc. Natl. Acad. Sci. USA*. 93:10933–10938. http://dx.doi.org/10.1073/pnas.93.20.10933

Landsman, L., and S. Jung. 2007. Lung macrophages serve as obligatory intermediate between blood monocytes and alveolar macrophages. *J. Immunol.* 179:3488–3494.

Licht, T., L. Tsirulnikov, H. Reuveni, T. Yarnitzky, and S.A. Ben-Sasson. 2003. Induction of pro-angiogenic signaling by a synthetic peptide derived from the second intracellular loop of S1P3 (EDG3). *Blood*. 102:2099–2107. http://dx.doi.org/10.1182/blood-2002-12-3634

Lin, E.Y., A.V. Nguyen, R.G. Russell, and J.W. Pollard. 2001. Colony-stimulating factor 1 promotes progression of mammary tumors to malignancy. *J. Exp. Med.* 193:727–740. http://dx.doi.org/10.1084/jem.193.6.727

Lin, E.Y., J.F. Li, L. Gnatovskiy, Y. Deng, L. Zhu, D.A. Grzesik, H. Qian, X.N. Xue, and J.W. Pollard. 2006. Macrophages regulate the angiogenic switch in a mouse model of breast cancer. *Cancer Res.* 66:11238–11246. http://dx.doi.org/10.1158/0008-5472.CAN-06-1278

Lyden, D., K. Hattori, S. Dias, C. Costa, P. Blaikie, L. Butros, A. Chadburn, B. Heissig, W. Marks, L. Witte, et al. 2001. Impaired recruitment of bone-marrow-derived endothelial and hematopoietic precursor cells blocks tumor angiogenesis and growth. *Nat. Med.* 7:1194–1201. http://dx.doi.org/10.1038/nm1101-1194

Mack, M., J. Cihak, C. Simonis, B. Luckow, A.E. Proudfoot, J. Plachý, H. Brühl, M. Frink, H.J. Anders, V. Vielhauer, et al. 2001. Expression and characterization of the chemokine receptors CCR2 and CCR5 in mice. *J. Immunol.* 166:4697–4704.

Matthews, V., B. Schuster, S. Schütze, I. Bussmeyer, A. Ludwig, C. Hundhausen, T. Sadowski, P. Saftig, D. Hartmann, K.J. Kallen, and S. Rose-John. 2003. Cellular cholesterol depletion triggers shedding of the human interleukin-6 receptor by ADAM10 and ADAM17 (TACE). *J. Biol. Chem.* 278:38829–38839. http://dx.doi.org/10.1074/jbc.M210584200

Nahrendorf, M., F.K. Swirski, E. Aikawa, L. Stangenberg, T. Wurdinger, J.L. Figueiredo, P. Libby, R. Weissleder, and M.J. Pittet. 2007. The healing myocardium sequentially mobilizes two monocyte subsets with divergent and complementary functions. *J. Exp. Med.* 204:3037–3047. http://dx.doi.org/10.1084/jem.20070885

Nissanov, J., R.W. Tuman, L.M. Gruver, and J.M. Fortunato. 1995. Automatic vessel segmentation and quantification of the rat aortic ring assay of angiogenesis. *Lab. Invest.* 73:734–739.

Palframan, R.T., S. Jung, G. Cheng, W. Weninger, Y. Luo, M. Dorf, D.R. Littman, B.J. Rollins, H. Zweerink, A. Rot, and U.H. von Andrian. 2001. Inflammatory chemokine transport and presentation in HEV: a remote control mechanism for monocyte recruitment to lymph nodes in inflamed tissues. *J. Exp. Med.* 194:1361–1373. http://dx.doi.org/10.1084/jem.194.9.1361

Peters, B.A., L.A. Diaz, K. Polyak, L. Meszler, K. Romans, E.C. Guinan, J.H. Antin, D. Myerson, S.R. Hamilton, B. Vogelstein, et al. 2005. Contribution of bone marrow-derived endothelial cells to human tumor vasculature. *Nat. Med.* 11:261–262. http://dx.doi.org/10.1038/nm1200

Phng, L.K., and H. Gerhardt. 2009. Angiogenesis: a team effort coordinated by notch. *Dev. Cell*. 16:196–208. http://dx.doi.org/10.1016/j.devcel.2009.01.015

Pipp, F., M. Heil, K. Issbrücker, T. Ziegelhoeffer, S. Martin, J. van den Heuvel, H. Weich, B. Fernandez, G. Golomb, P. Carmeliet, et al. 2003. VEGFR-1-selective VEGF homologue PlGF is arteriogenic: evidence for a monocyte-mediated mechanism. *Circ. Res.* 92:378–385. http://dx.doi.org/10.1161/01.RES.0000057997.77714.72

Pucci, F., M.A. Venneri, D. Biziato, A. Nonis, D. Moi, A. Sica, C. Di Serio, L. Naldini, and M. De Palma. 2009. A distinguishing gene signature shared by tumor-infiltrating Tie2-expressing monocytes, blood "resident" monocytes, and embryonic macrophages suggests common functions and developmental relationships. *Blood*. 114:901–914. http://dx.doi.org/10.1182/blood-2009-01-200931

Purhonen, S., J. Palm, D. Rossi, N. Kaskenpää, I. Rajantie, S. Ylä-Herttuala, K. Alitalo, I.L. Weissman, and P. Salven. 2008. Bone marrow-derived circulating endothelial precursors do not contribute to vascular endothelium and are not needed for tumor growth. *Proc. Natl. Acad. Sci. USA*. 105:6620–6625. http://dx.doi.org/10.1073/pnas.0710516105

Qian, B.Z., and J.W. Pollard. 2010. Macrophage diversity enhances tumor progression and metastasis. *Cell*. 141:39–51. http://dx.doi.org/10.1016/j.cell.2010.03.014

Ramachandran, P., A. Pellicoro, M.A. Vernon, L. Boulter, R.L. Aucott, A. Ali, S.N. Hartland, V.K. Snowdon, A. Cappon, T.T. Gordon-Walker, et al. 2012. Differential Ly-6C expression identifies the recruited macrophage phenotype, which orchestrates the regression of murine liver fibrosis. *Proc. Natl. Acad. Sci. USA*. 109:E3186–E3195. http://dx.doi.org/10.1073/pnas.1119964109

Ruzinova, M.B., R.A. Schoer, W. Gerald, J.E. Egan, P.P. Pandolfi, S. Rafii, K. Manova, V. Mittal, and R. Benezra. 2003. Effect of angiogenesis inhibition by Id loss and the contribution of bone-marrow-derived endothelial cells in spontaneous murine tumors. *Cancer Cell*. 4:277–289. http://dx.doi.org/10.1016/S1535-6108(03)00240-X

Sawano, A., S. Iwai, Y. Sakurai, M. Ito, K. Shitara, T. Nakahata, and M. Shibuya. 2001. Flt-1, vascular endothelial growth factor receptor 1, is a novel cell surface marker for the lineage of monocyte-macrophages in humans. *Blood*. 97:785–791. http://dx.doi.org/10.1182/blood.V97.3.785

Schaper, W. 2009. Collateral circulation: past and present. *Basic Res. Cardiol.* 104:5–21. http://dx.doi.org/10.1007/s00395-008-0760-x

Schaper, J., R. König, D. Franz, and W. Schaper. 1976. The endothelial surface of growing coronary collateral arteries. Intimal margination and diapedesis of monocytes. A combined SEM and TEM study. *Virchows Arch. A Pathol. Anat. Histol.* 370:193–205. http://dx.doi.org/10.1007/BF00427580

Schubert, S.Y., A. Benarroch, J. Ostvang, and E.R. Edelman. 2008. Regulation of endothelial cell proliferation by primary monocytes. *Arterioscler. Thromb. Vasc. Biol.* 28:97–104. http://dx.doi.org/10.1161/ATVBAHA.107.157537

Shojaei, F., X. Wu, A.K. Malik, C. Zhong, M.E. Baldwin, S. Schanz, G. Fuh, H.P. Gerber, and N. Ferrara. 2007. Tumor refractoriness to anti-VEGF treatment is mediated by CD11b+Gr1+ myeloid cells. *Nat. Biotechnol.* 25:911–920. http://dx.doi.org/10.1038/nbt1323

Shojaei, F., X. Wu, X. Qu, M. Kowanetz, L. Yu, M. Tan, Y.G. Meng, and N. Ferrara. 2009. G-CSF-initiated myeloid cell mobilization and angiogenesis mediate tumor refractoriness to anti-VEGF therapy in mouse models. *Proc. Natl. Acad. Sci. USA*. 106:6742–6747. http://dx.doi.org/10.1073/pnas.0902280106

Sica, A., P. Larghi, A. Mancino, L. Rubino, C. Porta, M.G. Totaro, M. Rimoldi, S.K. Biswas, P. Allavena, and A. Mantovani. 2008. Macrophage polarization in tumour progression. *Semin. Cancer Biol.* 18:349–355. http://dx.doi.org/10.1016/j.semcancer.2008.03.004

Swirski, F.K., M. Nahrendorf, M. Etzrodt, M. Wildgruber, V. Cortez-Retamozo, P. Panizzi, J.L. Figueiredo, R.H. Kohler, A. Chudnovskiy, P. Waterman, et al. 2009. Identification of splenic reservoir monocytes and their deployment to inflammatory sites. *Science*. 325:612–616. http://dx.doi.org/10.1126/science.1175202

Takeda, Y., S. Costa, E. Delamarre, C. Roncal, R. Leite de Oliveira, M.L. Squadrito, V. Finisguerra, S. Deschoemaeker, F. Bruyère, M. Wenes, et al. 2011. Macrophage skewing by Phd2 haplodeficiency prevents ischaemia by inducing arteriogenesis. *Nature*. 479:122–126. http://dx.doi.org/10.1038/nature10507

van Furth, R., J.A. Raeburn, and T.L. van Zwet. 1979. Characteristics of human mononuclear phagocytes. *Blood*. 54:485–500.

Varol, C., L. Landsman, D.K. Fogg, L. Greenshtein, B. Gildor, R. Margalit, V. Kalchenko, F. Geissmann, and S. Jung. 2007. Monocytes give rise to mucosal, but not splenic, conventional dendritic cells. *J. Exp. Med.* 204:171–180. http://dx.doi.org/10.1084/jem.20061011

Varol, C., A. Vallon-Eberhard, E. Elinav, T. Aychek, Y. Shapira, H. Luche, H.J. Fehling, W.D. Hardt, G. Shakhar, and S. Jung. 2009. Intestinal lamina propria dendritic cell subsets have different origin and functions. *Immunity*. 31:502–512. http://dx.doi.org/10.1016/j.immuni.2009.06.025

Yona, S., R. Hayhoe, and I. Avraham-Davidi. 2010. Monocyte and neutrophil isolation and migration assays. *Curr. Protoc. Immunol.* Chapter 14:Unit 14 15.

Yona, S., and S. Jung. 2010. Monocytes: subsets, origins, fates and functions. *Curr. Opin. Hematol.* 17:53–59.

Yona, S., K.W. Kim, Y. Wolf, A. Mildner, D. Varol, M. Breker, D. Strauss-Ayali, S. Viukov, M. Guilliams, A. Misharin, et al. 2012. Fate Mapping Reveals Origins and Dynamics of Monocytes and Tissue Macrophages under Homeostasis. *Immunity*. 38:79–91.

Zouggari, Y., H. Ait-Oufella, L. Waeckel, J. Vilar, C. Loinard, C. Cochain, A. Récalde, M. Duriez, B.I. Levy, E. Lutgens, et al. 2009. Regulatory T cells modulate postischemic neovascularization. *Circulation*. 120:1415–1425. http://dx.doi.org/10.1161/CIRCULATIONAHA.109.875583